



Combustion synthesis and electrochemical performance of $\text{Li}_2\text{FeSiO}_4/\text{C}$ cathode material for lithium-ion batteries

Mohammed Dahbi*, Sigita Urbonaite¹, Torbjörn Gustafsson

Department of Materials Chemistry, Ångström Advanced Battery Centre, Uppsala University, Box 538, SE-751 21 Uppsala, Sweden

ARTICLE INFO

Article history:

Received 22 October 2011

Received in revised form 10 January 2012

Accepted 12 January 2012

Available online 21 January 2012

Keywords:

Lithium-ion batteries

Lithium iron orthosilicate

Combustion synthesis

ABSTRACT

A novel preparation technique was developed for synthesizing $\text{Li}_2\text{FeSiO}_4/\text{C}$ nanoparticles through combustion of reaction mixtures containing silicon source, Li and Fe sources that operate as oxidizers and sucrose that act as a fuel. A systematic investigation of the synthesis parameters, such as the effect of the fuel content, on purity, morphology and electrochemical properties of the samples was performed. The samples were analyzed by X-ray diffraction (XRD), scanning electron microscopy (SEM), transmission electron microscopy (TEM), specific surface area (BET) and electrochemical measurements, respectively. Among the synthesized cathode materials, $\text{Li}_2\text{FeSiO}_4$ obtained with 1.5 mol of sucrose, showed the best electrochemical performance in terms of discharge capacity, cycling stability and rate capability. Discharge capacity of 130 mAh/g at C/20, 88 mAh/g at C/2 and 44 mAh/g at 2C were obtained with no capacity fading after 50 cycles.

© 2012 Elsevier B.V. All rights reserved.

1. Introduction

Lithium iron orthosilicate, $\text{Li}_2\text{FeSiO}_4$, has increasingly become a material of interest as a cathode for lithium ion batteries due to its promising electrochemical properties demonstrated the first time by Nyten et al. and the low cost compared to the cobalt based cathodes [1,2]. A limiting factor with polyanion materials is, however, their poor conductivity which can be mitigated by the introduction of a conductive carbon coating [3], particle size reduction [4], and supervalent cation doping [5]. Synthesis conditions have as expected a large influence on the electrochemical performances of $\text{Li}_2\text{FeSiO}_4$, and many studies have been performed to find out the key factor for optimized electrochemical performances [6–8]. Recent trends on $\text{Li}_2\text{FeSiO}_4$ are focused on development of active materials with nano-sized particle to improve the electrochemical performance by different synthesis techniques such as solid-state [1,9,10], sol–gel [11–13], hydrothermal [12], and hydrothermal assisted sol–gel [14]. Reducing the particle size is an effective way of increasing the surface area and decreasing the diffusion distance for charge transfer. In this investigation, we have developed a new, cheaper and rapid sucrose-aided combustion method, which is adequate for preparing homogeneous nano-sized

materials. Many cathode materials, such as LiCoO_2 [15], LiNiO_2 [16], $\text{LiNi}_{0.7-y}\text{Co}_{0.3-y}\text{Mn}_2\text{yO}_2$ [17,18] and LiMn_2O_4 [19], which were synthesized using the combustion process have showed an improved electrochemical performance. This method is based on an oxidation–reduction reaction between soluble precursor salts (oxidizers) and sacrificial, most often carbonaceous compounds (fuels). Most generally, a combustion reaction is controlled by several basic parameters: type of fuel and oxidizer, fuel-to-oxidizer molar ratio, ignition temperature, and relative volume of the evolved gaseous products. The most commonly used as oxidizer in this process is nitrates and urea or sucrose have been used as fuels [15,17,19]. We have now, for the first time, applied this method using metal nitrates as oxidizers and sucrose as fuel, to synthesis inexpensive and nano-sized silicate cathode material.

In this paper, a simple combustion method based on sucrose is employed to synthesize pure $\text{Li}_2\text{FeSiO}_4/\text{C}$ and improve the cycling performance of this silicate cathode material. This is a method which offers good sample homogeneity and allows synthesizing samples with small particle size. $\text{Li}_2\text{FeSiO}_4/\text{C}$ was prepared with various amounts of sucrose in order to optimize its electrochemical performances and to find out if this material can be used as possible alternative to LiCoO_2 and LiFePO_4 in lithium ion batteries.

2. Experimental

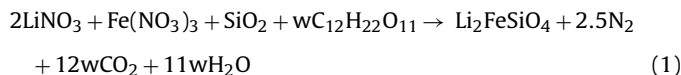
$\text{Li}_2\text{FeSiO}_4/\text{C}$ samples were prepared by the combustion method using LiNO_3 (Sigma–Aldrich) and $\text{Fe}(\text{NO}_3)_3 \cdot 9\text{H}_2\text{O}$ (Sigma–Aldrich)

* Corresponding author.

E-mail address: mohammed.dahbi@mkem.uu.se (M. Dahbi).

¹ Present address: Electrochemistry Laboratory, Paul Scherrer Institute, CH-5232 Villigen PSI, Switzerland.

as the oxidant precursors, sucrose (Sigma) as fuel and SiO₂ nanoparticles (Sigma) as silicon source. Typically, the reaction can be described as follows:



The stoichiometric amounts of reagent grade Li, Fe and Si sources were dissolved in the minimum amount of distilled water; the fuel (sucrose) was then added to the solution. The beaker containing the reaction mixture was placed on an electric heater and kept at 120 °C for 2 h to evaporate the excess water. The liquid adopted a syrup consistency and the colour changed from red to green while the syrup swelled up and transformed into brown foam. On continuing heating, this foamy mass started to burn spontaneously without flame and transformed finally to light and downy brownish-black powder. The as-formed powder was collected, ground in an agate mortar, and further heat-treated at 800 °C for 10 h under a flowing gas mixture (CO/CO₂: 50/50) to prevent the oxidation of Fe²⁺ cation.

In Eq. (1), the oxidizing valence of LiNO₃ is 10, that for Fe(NO₃)₃ is 15, whereas the reducing valence of the sucrose is 48 [20]. To keep the ratio between oxidizing and reducing valence equal to 1.0, we need to keep the stoichiometric parameter, *w*, in Eq. (1) equal to (10+15)/48 ≈ 0.5. To optimize the synthesis conditions, experiments were also carried out with other stoichiometric (*w*=1; 1.5; 2; 2.5 and 3) mol of sucrose. The samples thus prepared are referred to hereafter as 0.5Sc, 1Sc, 1.5Sc, 2Sc, 2.5Sc and 3Sc, where the coefficient denotes the parameter *w* and Sc stands for sucrose.

All samples were characterized by X-ray diffraction (XRD) using a Siemens D5000 diffractometer with Cu Kα radiation. The diffraction patterns were recorded in [10–120]° (*2θ*) angular range, using a 0.02° (*2θ*) step and a constant counting time of 10 s. The lattice parameters and cation distributions were refined by the Rietveld method using the Fullprof program [21].

The morphology of the samples was observed using a high resolution scanning electron microscopy (HRSEM LEO 1550). Transmission electron microscopy (TEM) studies were performed on JEOL JEM-2100F microscope, equipped with field emission gun operated at 200 kV. Specific surface area measurements were carried out by the Brunauer, Emmet and Teller (BET) method with a Micrometrics ASAP 2020 Accelerated Surface Area and Porosimetry Analyzer. Samples were dried 10 h at 300 °C under nitrogen before measurement. The Carbon content was calculated from thermogravimetric analysis (TGA) using TA instruments Q500, with a 10 °C min⁻¹ heating rate under a purified air flow in the temperature range between 25° and 600 °C.

Electrochemical measurements were performed in aluminium pouch cells. Positive electrodes were prepared by spreading a mixture of 75% active material, 15% carbon black, and 10% of PVDF [poly(vinylidene fluoride)] dissolved in NMP (1-methyl-2-pyrrolidinone) onto an aluminium foil. Circular electrodes (area: 3.14 cm²) were dried under vacuum at 120 °C in an argon-filled glove box (<3 ppm H₂O and O₂) before cell assembly. Batteries comprising the dried positive electrode, a glass fibre separator soaked in electrolyte and a lithium metal counter electrode (0.38 mm thick) were assembled and packed in the polymer-coated aluminium pouch in a so-called “Coffee-bag” configuration [22]. The electrolyte was 1 M LiPF₆ (Tomyama, dried over night at 80 °C in a vacuum furnace in the glove box) in an EC/DEC (Merck, battery grade and used as received) 2:1 by volume mixture. Charge–discharge tests were performed using a Digatron BTS600 battery testing system with different rates at 60 °C.

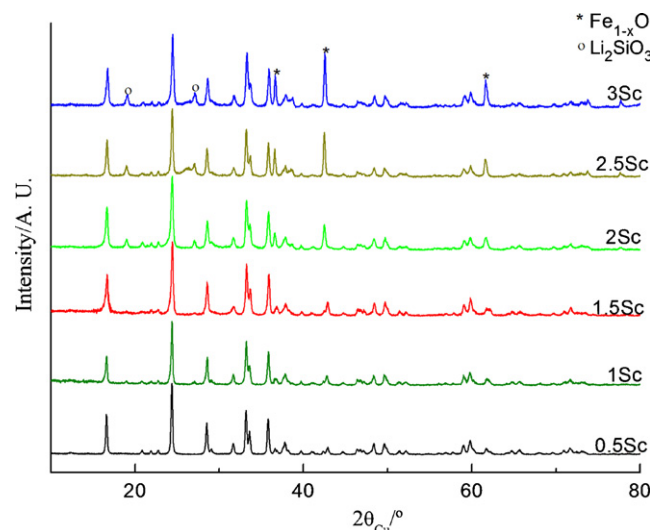


Fig. 1. X-ray diffraction patterns of Li₂FeSiO₄/C materials synthesized with different amounts of sucrose (0.5Sc, 1Sc, 1.5Sc, 2Sc, 2.5Sc and 3Sc).

3. Results and discussion

3.1. Structural characterizations

X-ray diffraction patterns of Li₂FeSiO₄/C composites (0.5Sc, 1Sc, 1.5Sc, 2Sc, 2.5Sc and 3Sc) are compared in Fig. 1. All the diffraction peaks can be indexed in a monoclinic cell (P₂₁/n space group) with the cell parameters *a* ~ 8.22 Å, *b* ~ 5.01 Å, *c* ~ 8.24 Å and β ~ 99.13 (see Table 1). Two impurities have been detected in the samples, and they are mainly Fe_{1-x}O and a small amount of Li₂SiO₃. A comparison of the diffraction patterns for the Li₂FeSiO₄/C composites with various amounts of sucrose shows that increasing sucrose content leads to increasing Fe_{1-x}O and Li₂SiO₃ impurities.

In order to accurately determine the structure of these materials, refinements by Rietveld method of X-ray data was performed using the Fullprof program [21]. The Rietveld refinement was used to determine the lattice and structural parameters as well as the cationic distribution between the lithium and iron sites.

Firstly, a full pattern matching refinement allowed determining the lattice parameters and the profile parameters of the Pseudo-Voigt function used to describe the shape of the diffraction lines. Then, the structural refinement was carried out by considering that the structure of Li₂FeSiO₄/C composites can be indexed in a monoclinic cell (P₂₁/n space group). As described in the P₂₁/n space group, the Li, Fe, Si, and O occupy 4e sites. All the crystallographic sites were constrained to be fully occupied. The isotropic atomic displacement parameters (Biso (Å²)) were refined. Cell parameters obtained for the six-Li₂FeSiO₄/C composites are compared in Table 1. These refinements of the cell and structural parameters are very close to those reported by Nishimura et al. [10] (*a* = 8.230(2) Å, *b* = 5.021(2) Å, *c* = 8.234(2) Å, and β = 99.232(3)) but we used the P₂₁/n space group instead of P₂₁. Detailed results of the X-ray diffraction pattern refinement by Rietveld method are given as example in Table 2 for 0.5Sc, whereas Fig. 2 gives a comparison of the experimental and calculated XRD patterns. A good minimization of the difference (*I*_{obs.} – *I*_{cal.}) with low Rietveld agreement factors (*R*_{wp} = 10.9%; *R*_B = 4.97%) indicates a good description of the structure in the P₂₁/n space group.

The possible antisite defect between lithium and iron ions in the 4e sites was also checked (see Table 2). The refinement of all our XRD patterns assuming this structural hypothesis, i.e. P₂₁/n space group, shows that no cation mixing between the Li and Fe ions.

Table 1
Comparison of cell parameters obtained by the Rietveld refinement, BET surface area, crystallite size and carbon content for the $\text{Li}_2\text{FeSiO}_4/\text{C}$ samples as the amount of sucrose is increased.

Sample	a (Å)	b (Å)	c (Å)	β	S_{BET} ($\text{m}^2 \text{g}^{-1}$)	Crystallite size ^a (nm)	Carbon content (%)
0.5Sc	8.2274(3)	5.0175(2)	8.2313(2)	99.1308(2)	3.66	43	0.76
1Sc	8.2220(3)	5.0137(2)	8.2363(3)	99.1303(3)	9.67	41	5.44
1.5Sc	8.2207(1)	5.0171(2)	8.2445(2)	99.0758(2)	59.75	29	11.38
2Sc	8.2212(2)	5.0198(3)	8.2467(4)	99.0493(3)	74.54	27	18
2.5Sc	8.2255(1)	5.0198(2)	8.2498(3)	99.1632(3)	91.31	25	20.63
3Sc	8.2252(3)	5.0144(2)	8.2501(2)	99.2277(2)	117.47	23	21.05

^a The average crystallite size was estimated from the full width at half maximum (FWHM) of diffraction line (111) considering the Scherrer formula $\text{FWHM}(2\theta) = 0.9\lambda / (L \cos\theta)$ with $\lambda = 1.54 \text{ \AA}$ for the $\text{K}\alpha$ Cu radiation and L the average crystallite size.

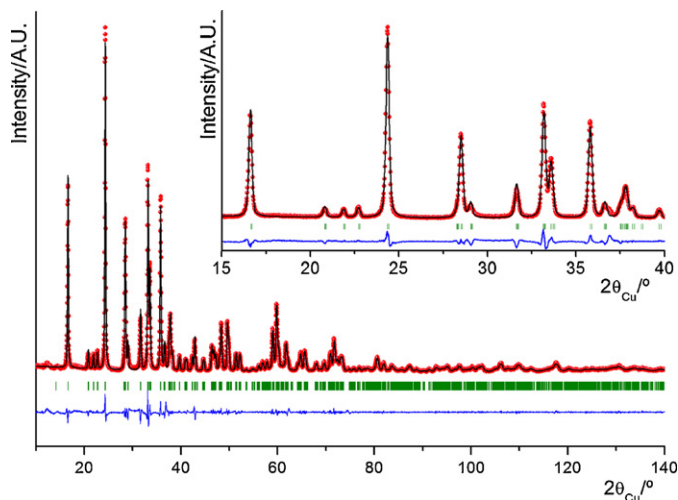


Fig. 2. Rietveld refinement of X-ray diffraction pattern obtained for $\text{Li}_2\text{FeSiO}_4/\text{C}$ material with 0.5Sc of sucrose. Detailed diffraction data in the 15–40° range is shown as an inset.

3.2. Textural characterizations

High resolution scanning electron microscopy was used to check trends in powder grain size and morphology with increasing sucrose amount. Fig. 3 gives a comparison of SEM micrographs

obtained for the $\text{Li}_2\text{FeSiO}_4/\text{C}$ materials with various amount of sucrose (0.5Sc, 1.5Sc, 2Sc and 3Sc). In the sample prepared with a low amount of sucrose (0.5Sc), there was a greater extent of aggregation of particles, and it had a larger particle size distribution. By increasing the amount of sucrose, a significant decrease in particle size and a more uniform particle size distribution are observed.

To determine the carbon content in the $\text{Li}_2\text{FeSiO}_4/\text{C}$ samples, we used TGA method to measure the amount of carbon released from the samples during the temperature scan under air flow. As example, Fig. 4 shows the TGA curves performed on both 0.5Sc and 1Sc, respectively. The TGA curves show a weight gain of 4.18% for the sample 0.5Sc and a weight loss of 0.54% for 1Sc sample. Based on the assumption that, in the temperature range of 200–600 °C, $\text{Li}_2\text{FeSiO}_4$ is oxidized to Li_2SiO_3 and Fe_2O_3 , corresponding to a theoretical weight gain of 4.9%. As for 1Sc, when the sample is heated above 360 °C, the carbon in the mixture is oxidized to CO_2 gas, leading to a weight loss. Above 600 °C, a total oxidation of both $\text{Li}_2\text{FeSiO}_4$ and carbon is completed. Finally, by taking into account the theoretical weight gain (4.9%) of pure $\text{Li}_2\text{FeSiO}_4$ during TGA measurement, the amounts of coated carbon for the 0.5Sc and 1Sc samples were calculated to be ~0.72% (almost without carbon) and ~5.44%, respectively.

The crystallite size and the specific surface area of all samples were also estimated by XRD and BET method, respectively. Table 1 gives all results for $\text{Li}_2\text{FeSiO}_4/\text{C}$ samples at various quantities of sucrose. As shown in this table, with increasing of sucrose quantities, the surface area increased while the crystallite size

Table 2
Structural and profile parameters obtained by Rietveld refinement of the X-ray diffraction pattern recorded for 0.5Sc sample.

Space group: $P2_1/n$							
$a = 8.2274(3) \text{ \AA}$							
$b = 5.0175(2) \text{ \AA}$							
$c = 8.2313(2) \text{ \AA}$							
$\beta = 99.1308(2)$							
Atom	Wyckoff	x	y	z	B (\AA^2)	Occupancy	
Li_1	4e	0.6420(2)	0.8771(4)	0.6813(2)	1.250(1)	1.00	
		0.6417(2) ^a	0.8803(4) ^a	0.6829(1) ^a	0.960(2) ^a	0.986Li/0.014Fe ^a	
Li_2	4e	0.5877(1)	0.2224(2)	0.0584(1)	1.250(1)	1.00	
Fe	4e	0.2905(3)	0.8021(5)	0.5438(4)	0.802(3)	1.00	
		0.2911(2) ^a	0.8022(4) ^a	.5434(1) ^a	0.960(2) ^a	0.986Fe/0.014Li ^a	
Si	4e	0.0376(1)	0.8136(6)	0.7981(5)	0.249(1)	1.00	
O_1	4e	0.8534(1)	0.7294(2)	0.8325(1)	0.808(2)	1.00	
O_2	4e	0.4315(1)	0.2060(1)	0.8755(1)	0.868(2)	1.00	
O_3	4e	0.6839(4)	0.7611(2)	0.4444(1)	0.725(1)	1.00	
O_4	4e	0.9604(5)	0.8525(2)	0.2214(5)	1.499(1)	1.00	
Conditions of the run							
Temperature	300 K						
Angular range	$10^\circ \leq 2\theta \leq 140^\circ$						
Displacement sample holder (2θ)	0.0225						
Number of fitted parameters	56						
Conventional Rietveld R -factors for points with Bragg contribution							
$R_{\text{wp}} = 10.9\%$; $R_{\text{B}} = 4.97\%$							
$R_{\text{wp}} = 10.9\%$ ^a ; $R_{\text{B}} = 5.17\%$ ^a							

^a Obtained Rietveld results considering the antisite defect between lithium and iron ions.

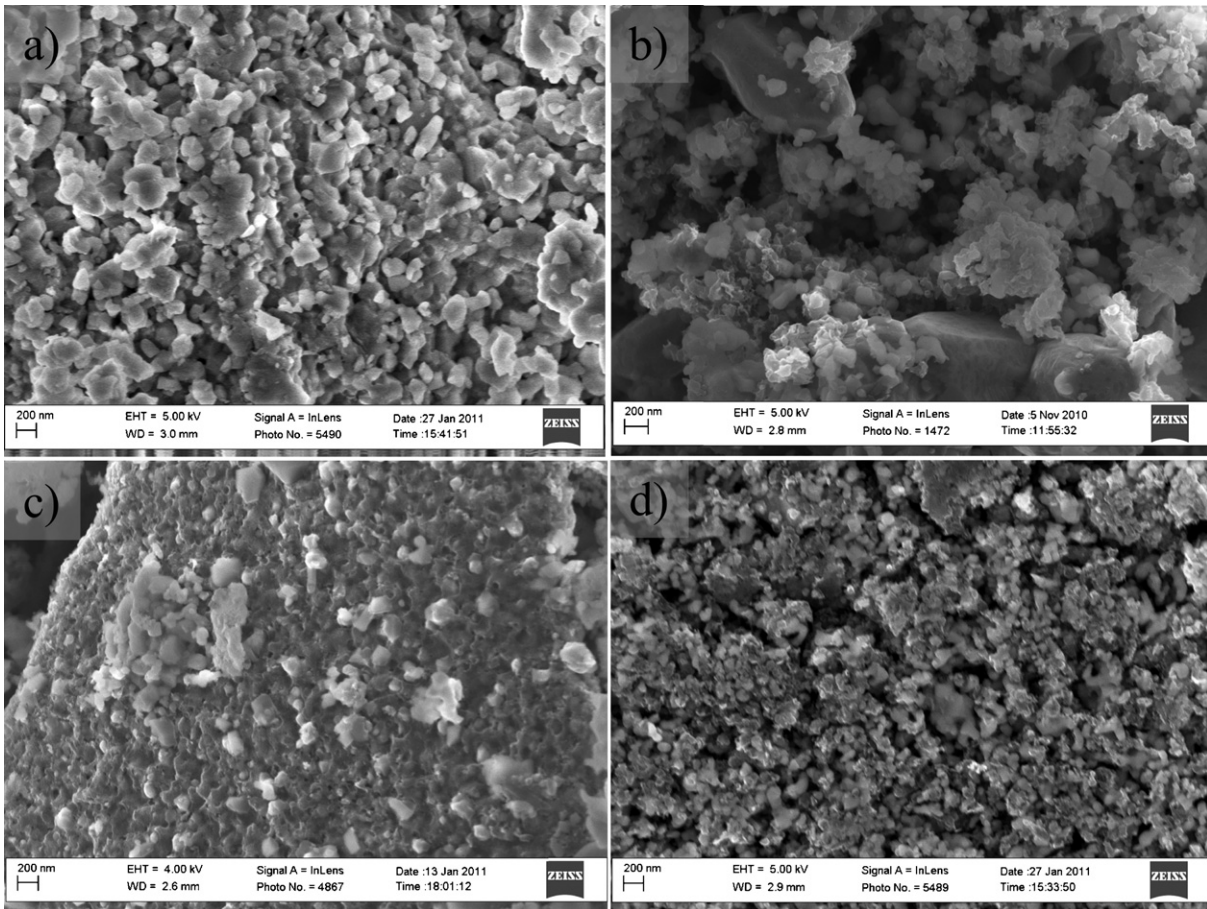


Fig. 3. SEM images of $\text{Li}_2\text{FeSiO}_4/\text{C}$ materials with various amounts of sucrose: (a) 0.5Sc, (b) 1.5Sc, (c) 2Sc and (d) 3Sc.

decreased. A proportion of the surface area (increase from 3.66 to $117.47 \text{ m}^2 \text{ g}^{-1}$) would be attributed to the increased levels of residual carbon (0.72–21.05%) in the samples. However, the presence of increasing amounts of sucrose also inhibits crystallite growth which results in higher surface areas of the active $\text{Li}_2\text{FeSiO}_4/\text{C}$ materials.

In order to study the effect of the amount of sucrose on the carbon coating, TEM observations were carried out and the results are presented in Fig. 5. It is clear that the samples show

different carbon distribution on $\text{Li}_2\text{FeSiO}_4$ particle surface. TEM images of samples 0.5Sc and 1Sc, containing only 0.72% and 5.44% carbon, respectively, do not provide information about carbon distribution, see Fig. 5(a–b), as the amount of carbon is too low to be detected. When the carbon content is increased to about 11.38% (1.5Sc), the carbon coating is comparatively uniform, and the conductive carbon spreads all over the particles. For samples 2.5Sc and 3Sc, although the active materials are also coated completely by carbon, there is also carbon agglomerates formed by excessive graphene-like carbon around particles. It can be concluded that the sucrose content is a critical factor for the carbon distribution around particles, and the surfaces cannot be coated effectively until the carbon content reaches a critical value (about 10%). Therefore, the presence of carbon always leads to a more uniform particle distribution and, consequently, higher conductivity and smaller particle size of $\text{Li}_2\text{FeSiO}_4/\text{C}$ composite materials. We can thus assume that the particles size or/and specific surface area, as well as carbon content could influence the electrochemical performance. For this reason, the electrochemical behaviour for these $\text{Li}_2\text{FeSiO}_4/\text{C}$ materials was investigated by galvanostatic cycling.

3.3. Electrochemical study

To clarify the effect of the amount of sucrose on the electrochemical performance of the $\text{Li}_2\text{FeSiO}_4/\text{C}$, some electrochemical tests were carried out. Fig. 6 shows the first discharge curves of the cells with various $\text{Li}_2\text{FeSiO}_4/\text{C}$ electrodes at C/20 rate over the potential range of 1.8–4.0 V. It can be seen that the initial discharge capacities of $\text{Li}_2\text{FeSiO}_4/\text{C}$ samples synthesized with different amounts of sucrose 0.5Sc, 1Sc, 1.5Sc, 2Sc, 2.5Sc and 3Sc are 30, 64, 135, 94,

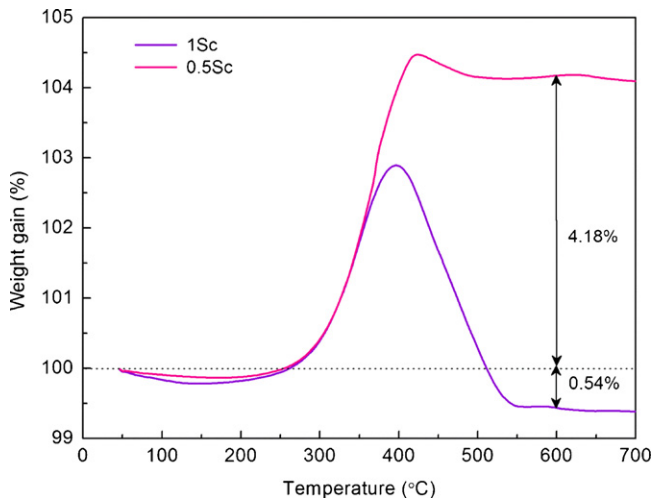


Fig. 4. TGA curves of 0.5Sc and 1Sc samples.

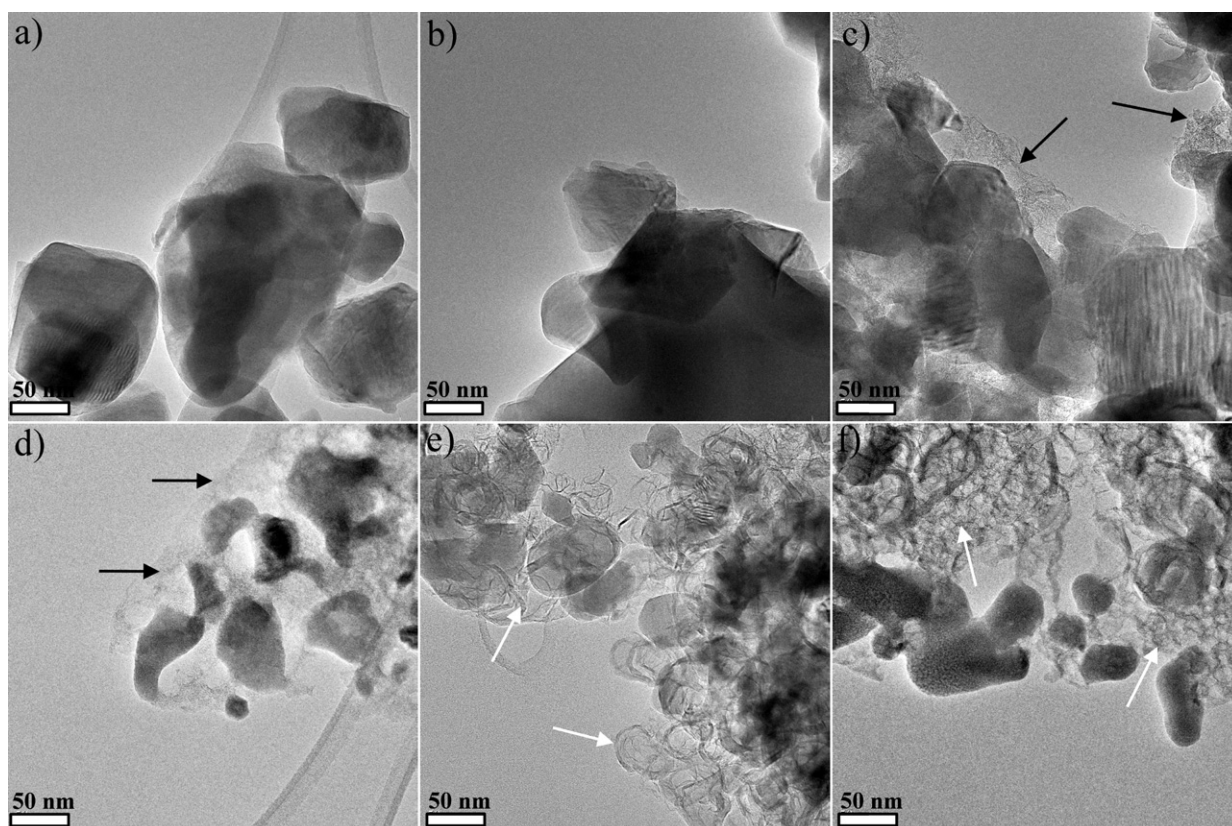


Fig. 5. TEM images of $\text{Li}_2\text{FeSiO}_4/\text{C}$ materials with various amounts of sucrose: (a) 0.5Sc, (b) 1Sc, (c) 1.5Sc, (d) 2Sc, (e) 2.5Sc and (f) 3Sc. The carbon and graphene are marked with black and white arrows, respectively.

111 and 92 mAh g^{-1} , respectively. From the XRD and BET measurements of the samples, we can explain why the $\text{Li}_2\text{FeSiO}_4/\text{C}$ powder prepared with 1.5Sc delivers the highest discharge capacity. It is known that good ionic transport (small particle size) and phase-pure material are two key factors to improve the electrochemical performance of $\text{Li}_2\text{FeSiO}_4$ [6–8]. As described in the previous section, particles of $\text{Li}_2\text{FeSiO}_4/\text{C}$ powder synthesized with low amounts of sucrose have low levels of impurities but also low specific surface area, indicating larger particle size, which is also supported by the diffraction experiment. This leads to a slow transport of

lithium ions to and from the particle core. On the other hand, increasing the amount of sucrose affects the purity of $\text{Li}_2\text{FeSiO}_4/\text{C}$ material and results in presence of two major impurities Li_2SiO_3 and Fe_{1-x}O . As a result, 1.5Sc is the optimum amount of sucrose for the $\text{Li}_2\text{FeSiO}_4/\text{C}$ with both high intrinsic conductivity due the carbon content ($\sim 12 \text{ wt}\%$) and an almost phase-pure material, which results in the best electrochemical performance. According to our results the 1.5Sc sample is the most outstanding one, and hence we have studied more electrochemical properties of that sample.

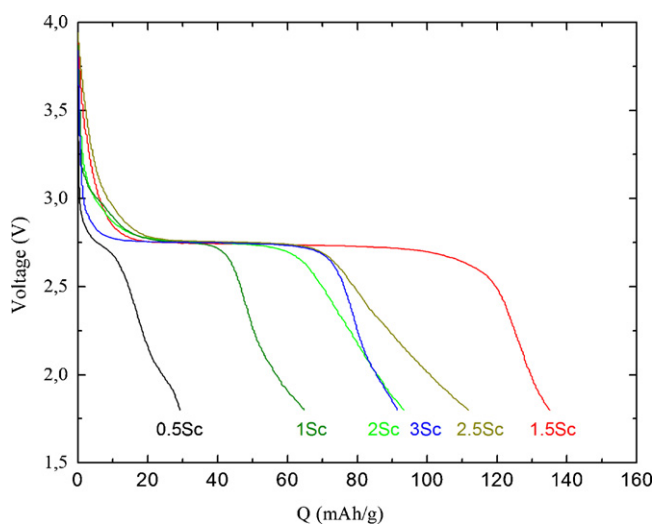


Fig. 6. The first discharge capacities for various $\text{Li}_2\text{FeSiO}_4/\text{C}$ cathodes synthesized at different amounts of sucrose.

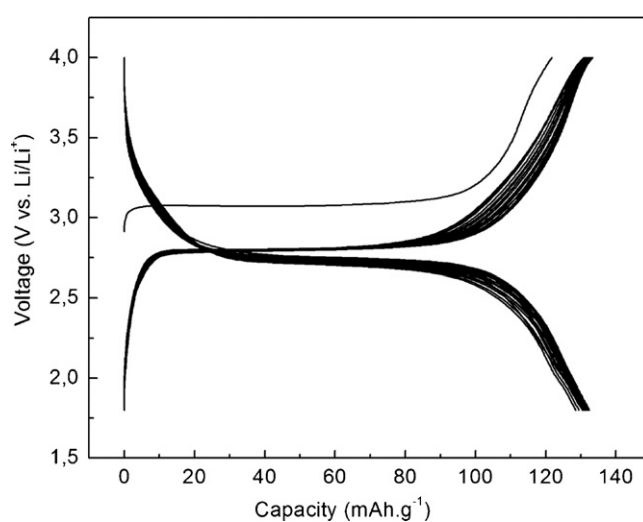


Fig. 7. Variation of the cell voltage vs. lithium amount at the C/20 rate for the first 50 galvanostatic charge/discharge cycles for 1.5Sc sample.

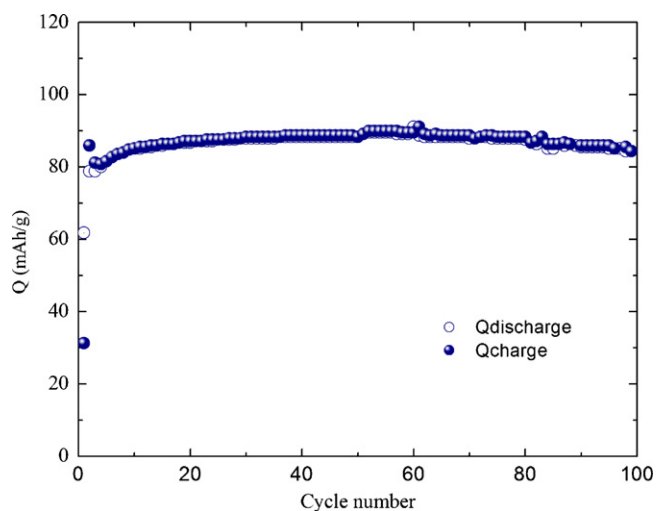


Fig. 8. Evolution of the charge and discharge capacity for a Li//Li₂FeSiO₄ (1.5Sc) cell during 100 cycles at the C/2 rate in the 1.8–4 V range.

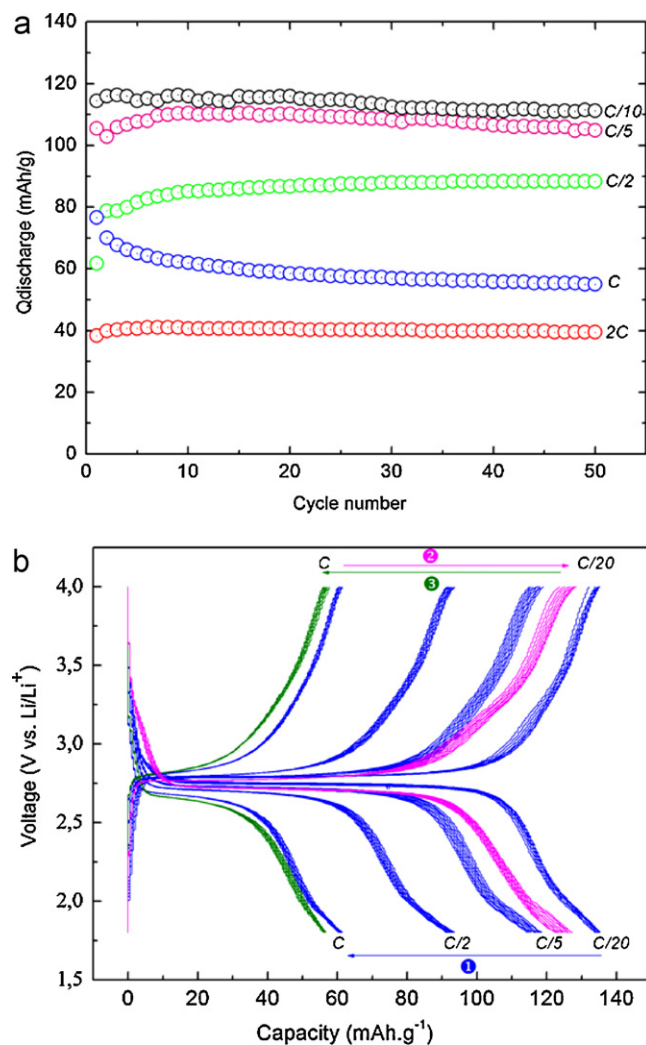


Fig. 9. Cyclic performance of Li₂FeSiO₄ (1.5Sc) cathode cycled between 1.8 and 4 V vs. Li/Li⁺ at: (a) different C/n rates over 50 cycles and (b) successive sequences of a 10 cycles at different C/n rates.

In order to determine the capacity and cyclability of 1.5Sc electrode, we performed charge/discharge cycling on Li₂FeSiO₄/C electrodes at different rates. Fig. 7 gives the change in voltage vs. lithium amount during the first fifty galvanostatic charge/discharge cycles performed between 1.8 and 4 V (vs. Li⁺/Li) at C/20 rate. It is seen that this sample shows a reversible capacity of 130 mAh/g, compared to the theoretical capacity of 166 mAh/g. A much higher charge potential was observed in the first cycle, which can indicate a phase transition to a more stable structure [1,2,14]. This very good reversibility is confirmed in Fig. 8 that gives the evolution of charge/discharge capacities at C/2 rate during the 100 cycles. Indeed, one can observe that the capacity remains above 88 mAh/g after 100 cycles at high rate. This high cyclability could be attributed to an enhanced electronic conductivity due to the presence of carbon and to a small particle size obtained by combustion method. Since the individual Li₂FeSiO₄ particles are connected by a carbon network, the active Li₂FeSiO₄/C materials can be fully utilized for lithium extraction and insertion reactions.

To characterize the material response to the change in cycling conditions, two different cycling modes were used. For the first one, the cycle performance of five independent cells was investigated for up to 50 cycles at different rates between C/10 to 2C. As seen in Fig. 9a, the discharge capacity dropped with increasing current density (C-rate) from 120 mAh/g to 88 mAh/g and 40 mAh/g at C/10, C/2 and 2C, respectively. For the second cycling mode with rate changes, sequences of charge/discharge cycles were successively performed at C/n rate, n could vary between 20 and 1. This cycling program was alternated between slow and fast cycling rates on one single cell. Fig. 9b shows the charge–discharge curves obtained for this Li₂FeSiO₄/C material used as positive electrode material in lithium cell cycled in this condition. This electrochemical test clearly shows that the capacity retention remains very good between C/20 to C rates, in good agreement with the results reported in Fig. 9a. Furthermore, stable reversible capacity at C/20 rate-comparable to that obtained initially-even after cycling at high rate (C rate for instance) during a few cycles.

To summarise, the good capability of the studied electrode material, even at higher rates, can be explained by the high surface area and small particle size formed by the combustion method.

4. Conclusion

Nano-sized Li₂FeSiO₄/C powders have been successfully synthesized by a novel combustion process in which a very low-cost material, sucrose, was used as fuel. As the sucrose amount increases from half-stoichiometric to triple stoichiometric, the purity and morphology of the products was affected. XRD analysis shows that the amount of Li₂SiO₃ and Fe_{1-x}O impurities increases with increasing sucrose amount. Combined SEM and TEM micrographs and BET analysis show that the addition of sucrose is favourable for increasing the surface area while the particle size decreased. The best electrochemical performance was reached for the sample with 1.5 mol of sucrose as compared to the other stoichiometric, which delivered an attractive capacity of 130 mAh/g at C/20 rate with stable cycling performance even at 2C, owing to the good crystallinity and phase purity.

Acknowledgements

The authors would like to thank the Swedish Research Council (VR), the Swedish Energy Agency (STEM) and the Global Climate and Energy Project (GCEP) of Stanford University for the financial support and Henrik Eriksson for the technical assistance.

References

- [1] A. Nytén, A. Abouimrane, M. Armand, T. Gustafsson, J.O. Thomas, *Electrochem. Commun.* 7 (2005) 156.
- [2] A. Nytén, S. Kamali, L. Häggström, T. Gustafsson, J.O. Thomas, *J. Mater. Chem.* 16 (2006) 2266.
- [3] H. Huang, S.-C. Yin, L.F. Nazar, *Electrochem. Solid-State Lett.* 4 (2001) A170.
- [4] C. Delacourt, P. Poizot, S. Levasseur, C. Masquelier, *Electrochem. Solid-State Lett.* 9 (2006) A352–A355.
- [5] S.Y. Chung, J.T. Bloking, Y.M. Chiang, *Nat. Mater.* 1 (2002) 123.
- [6] M. Nadherná, R. Dominko, D. Hanzel, J. Reiter, M. Gaberscek, *J. Electrochem. Soc.* 156 (2009) A619–A626.
- [7] Z.L. Gong, Y.X. Li, Y. Yang, *Electrochem. Solid-State Lett.* 9 (2006) A542–A544.
- [8] C. Deng, S. Zhang, B.L. Fu, S.Y. Yang, L. Ma, *Mater. Chem. Phys.* 120 (2010) 14–17.
- [9] K. Zaghib, A.A. Salah, N. Ravet, A. Mauger, F. Gendron, C.M. Julien, *J. Power Sources* 160 (2006) 1381.
- [10] S. Nishimura, S. Hayase, R. Kanno, M. Yashima, N. Nakayama, A. Yamada, *J. Am. Chem. Soc.* 130 (2008) 13212–13213.
- [11] R. Dominko, M. Bele, M. Gaberšček, A. Meden, M. Remškar, J. Jamnik, *Electrochem. Commun.* 8 (2006) 217.
- [12] R. Dominko, D.E. Conte, D. Hanze, M. Gaberscek, J. Jamnik, *J. Power Sources* 178 (2008) 842–847.
- [13] C. Deng, S. Zhang, S.Y. Yang, *J. Alloys Compd.* 487 (2009) L18–L23.
- [14] Z.L. Gong, Y.X. Li, G.N. He, J. Li, Y. Yang, *Electrochem. Solid-State Lett.* 11 (2008) A60.
- [15] E.I. Santiago, A.V.C. Andrade, C.O. Paiva-Santos, L.O.S. Bulhoes, *Solid State Ionics* 158 (2003) 91–102.
- [16] M.Y. Song, I.K. Kwon, H.U. Kim, S.B. Shim, D.R. Mumm, *J. Appl. Electrochem.* 36 (2006) 801.
- [17] M. Dahbi, I. Saadoune, J.M. Amarilla, *Electrochem. Acta* 53 (2008) 5266.
- [18] I. Saadoune, M. Dahbi, M. Wikberg, T. Gustafsson, P. Svedlindh, K. Edström, *Solid State Ionics* 178 (2008) 1668.
- [19] J.M. Amarilla, K. Petrov, F. Pico, G. Avdeev, J.M. Rojo, R.M. Rojas, *J. Power Sources* 191 (2009) 591–600.
- [20] N.A. Dhas, K.C. Patil, *J. Solid State Chem.* 102 (1993) 440–445.
- [21] J. Rodriguez-Carvajal, Fullprof, Program for Rietveld Refinement, version 3.7, LLB JRC, 1997.
- [22] T. Gustafsson, J.O. Thomas, R. Koksang, G.C. Farrington, *Electrochim. Acta* 37 (1992) 1639.